



# The nonlinear absorption properties of TaSe<sub>2</sub> and its application in ~ 2.0 μm pulsed solid-state lasers

Lulu Dong<sup>1</sup> · Mengxin Xue<sup>1</sup> · Junting Liu<sup>2</sup> · Kuan Li<sup>2</sup> · Jiawen Lv<sup>2</sup> · Yicheng Jin<sup>2</sup> · Shande Liu<sup>2</sup>

Received: 22 May 2024 / Accepted: 5 July 2024 / Published online: 12 July 2024  
© The Author(s), under exclusive licence to Springer-Verlag GmbH Germany, part of Springer Nature 2024

## Abstract

Enhancing the performance of saturable absorbers (SAs) crafted from two-dimensional (2D) narrow-bandgap materials is crucial for their use in ~ 2.0 μm pulse laser applications. In this context, a high-quality TaSe<sub>2</sub> SA was successfully fabricated by mechanical exfoliation. The TaSe<sub>2</sub> SA exhibited saturable absorption characteristics at around 2.0 μm, with a modulation depth of 7.1% and an unsaturated loss of 3.1%. Utilizing this newly fabricated SA, a passively Q-switched Tm:YAP laser operating near 2.0 μm was achieved. At the highest absorbed pump power of 5.58 W, the laser produced a maximum average output power of 1.34 W, with a pulse width measuring 550 ns at 89 kHz. This performance translates to a peak single pulse energy of 15.0 μJ and a maximum peak power of 27.27 W.

## 1 Introduction

~ 2.0 μm pulse lasers, crucial for deep tissue penetration and minimal scattering, are indispensable in advanced medical diagnostics and atmospheric sensing technologies [1–3]. Passive Q-switching technology is an effective method for generating pulsed lasers and employs a saturable absorber (SA) as a fundamental yet potent optical device that facilitates rapid transitions between absorption states, thus

producing short-pulse lasers [4]. Semiconductor saturable absorber mirror (SESAM), commonly used as an SA, has limited wavelength tuning capabilities due to complex fabrication and restricted nonlinear optical bandwidths. Since 2009, a diverse array of two-dimensional (2D) materials, such as graphene, black phosphorus (BP), transition metal dichalcogenides (TMDs), and MXenes, have been recognized for their superior nonlinear absorption characteristics [5–9]. These materials demonstrate immense promise as SA due to their broad bandwidth, high nonlinear absorption coefficients, adjustable modulation depth, and saturation intensity, along with ease of fabrication and integration. However, each 2D material also has its limitations employed as SA. For example, the modest absorptance (approximately 2.3% for a single layer) and sparse density of states in graphene impede the achievement of high modulation depths [5]. For TMDs, their extensive bandgaps restrict usage to visible and near-infrared spectra. Additionally, the principal challenge for real applications of BP and MXenes is their poor air stability [7, 9]. Consequently, there is an ongoing imperative to investigate novel 2D materials and structures to enhance the characteristics and efficacy of current saturable absorbers, thereby advancing the development of passive Q-switched lasers.

Recent investigations have demonstrated that 2H-TaSe<sub>2</sub> constitutes an air-stable, two-dimensional semiconductor with a narrow bandgap of approximately 0.15 eV. It demonstrates an ultrafast carrier saturation recovery time alongside a significant nonlinear absorption coefficient, positioning it

✉ Lulu Dong  
qut\_lulu@163.com  
Mengxin Xue  
mengxinxue0902@163.com  
Junting Liu  
jtliu\_sdust@163.com  
Kuan Li  
lk13853629173@163.com  
Jiawen Lv  
ljw1231204@163.com  
Yicheng Jin  
jin990515@163.com  
Shande Liu  
pepsl\_liu@163.com

<sup>1</sup> School of Science, Qingdao University of Technology, Qingdao 266525, China

<sup>2</sup> College of Electronic and Information Engineering, Shandong University of Science and Technology, Qingdao 266590, China

as a viable candidate for an SA in pulse generation applications. While the utilization of TaSe<sub>2</sub> in generating solid-state pulsed lasers within the 3.0 μm wavelength band has been documented [10], its application for lasers operating in the ~2.0 μm remains hitherto unreported.

In this investigation, 2H-TaSe<sub>2</sub>, fabricated via mechanical exfoliation, was utilized as an SA in the Tm:YAP bulk lasers. The nonlinear absorption properties were analyzed using a nondegenerate pump-probe setup. Employing 2H-TaSe<sub>2</sub> as the SA, stable Q-switched pulse output was achieved. At an absorbed pump power of 5.58 W, the Q-switched laser delivered a peak output power of 1.34 W, corresponding to a slope efficiency of 28.3%. The minimal pulse duration achieved was 550 ns, at a frequency of 89 kHz. Consequently, the laser produced a maximum single pulse energy of 15.0 μJ and a peak pulse power of 27.27 W.

## 2 Preparation and characterization

### 2.1 Preparation and morphology characterization

High-quality TaSe<sub>2</sub> nanoplates were synthesized utilizing the mechanical exfoliation technique. Initially, layers were exfoliated from the TaSe<sub>2</sub> bulk material using Polydimethylsiloxane (PDMS) as the medium. The PDMS, embedded with the TaSe<sub>2</sub> layers, was subsequently placed onto a sapphire substrate. This assembly was then heated at 100 °C for two minutes on a heating table. Following the heating process, the PDMS was detached from the sapphire substrate,

facilitating the transfer of TaSe<sub>2</sub> nanoplates onto the sapphire surface.

At room temperature, 2H-TaSe<sub>2</sub> exhibits a hexagonal (P63/mmc) crystal structure composed of dual-layered Se-Ta-Se sandwiches aligned along the c-axis. In this arrangement, Ta atoms are centrally positioned within a trigonal prism, coordinated by six Se atoms [11]. Energy-dispersive X-ray spectroscopy (EDS) was employed to ascertain the chemical composition of the TaSe<sub>2</sub> powder. As depicted in Fig. 1a,b, the elemental map revealed a uniform distribution of Ta and Se. Additionally, the atomic ratio of Ta to Se, derived from the EDS spectrum shown in Fig. 1d, was approximately 1:2. The morphology of the TaSe<sub>2</sub> sample was analyzed through Atomic Force Microscopy (AFM), which indicated a nanosheet thickness of ~3 nm, as shown in Fig. 1c. The AFM findings further confirmed the high uniformity and continuity of the TaSe<sub>2</sub> nanosheets. Additionally, Raman spectroscopy identified one peaks at 114 cm<sup>-1</sup> (Fig. 1e), aligning with previously reported research [12].

### 2.2 Nonlinear absorption properties

The saturable absorption properties of the 2H-TaSe<sub>2</sub> were examined using an I-scan technique, employing a custom-built 2 ps Tm:YAP mode-locked laser operating at a repetition rate of 100 MHz. The laser output was concentrated to a minimal spot radius of 10 μm through a 10× objective lens. The observed nonlinear transmittance, presented in Fig. 2, was analyzed and fit using the following equation [13].

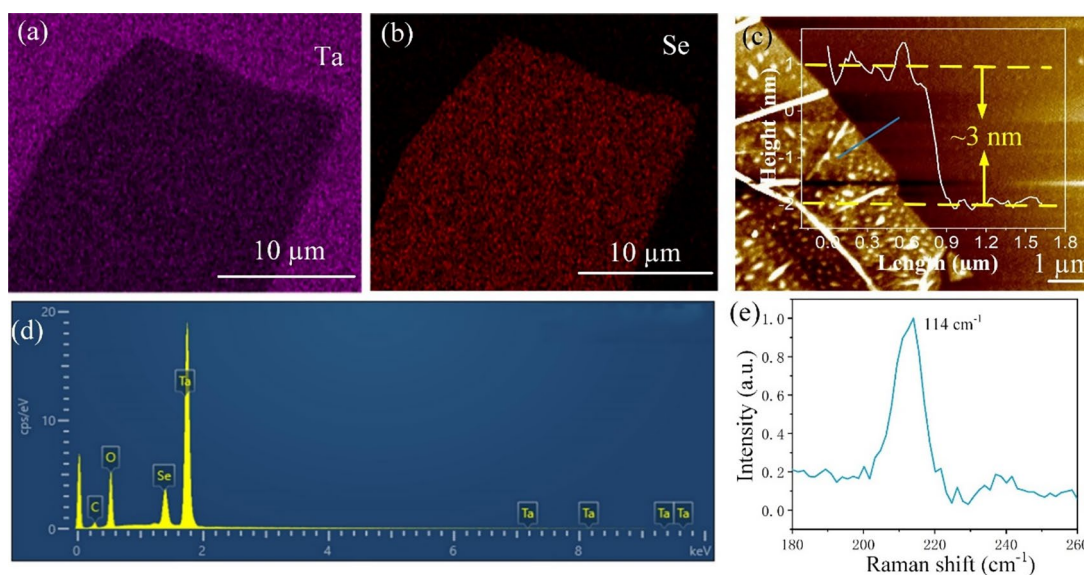


**Fig. 1** a, b EDS mapping images of Ta, and Se in TaSe<sub>2</sub>. (c) AFM image and typical height profiles. d EDS spectra. e Raman spectra of the 2H-TaSe<sub>2</sub>

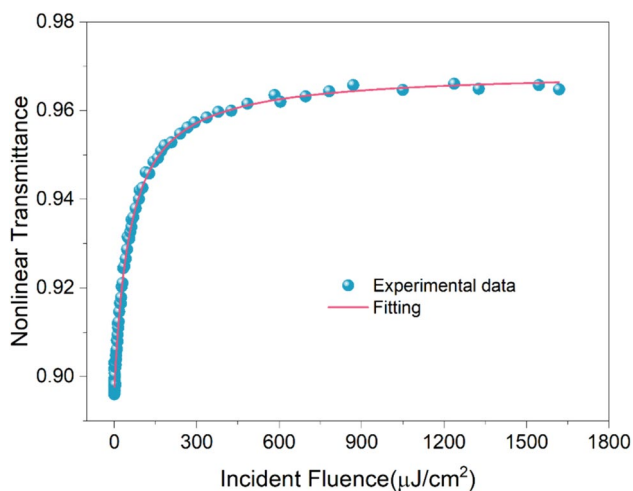


**Fig. 2** Nonlinear transmittance curve of TaSe<sub>2</sub> SA at 2.0 μm

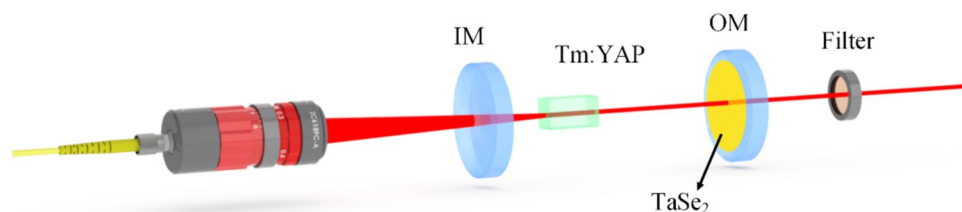
$$T = 1 - \frac{\Delta R}{1 + \Phi/\Phi_s} - A_{ns} \quad (1)$$

In the formula,  $\Delta R$ ,  $\Phi_s$ , and  $A_{ns}$  represent the modulation depth, saturation fluence, and nonsaturable loss, respectively. Analysis revealed that for TaSe<sub>2</sub> SA, the modulation depth was 7.1%, nonsaturable loss stood at 3.1%, and saturation fluence was determined to be 58.7 μJ/cm<sup>2</sup>. These findings highlight the superior nonlinear absorption capabilities of TaSe<sub>2</sub> SA at a wavelength of 2.0 μm.

### 3 Q-switched experimental setup

Figure 3 illustrates the schematic layout of the TaSe<sub>2</sub> Q-switched laser system, which consists of a concave Plano cavity measuring 20 mm in length. The gain medium utilized is a Tm:YAP crystal sized 3 × 3 × 8 mm<sup>3</sup>. The pumping mechanism involves a fiber-coupled diode laser with a central wavelength of 793 nm, featuring a numerical aperture (NA) of 0.22 and a core diameter of 200 μm. The pump light, collimated and focused to a diameter of 200 μm, is channeled through a 1:1 focusing system into the Tm:YAP crystal. The crystal is encased in indium foil to reduce thermal effects and mounted in a temperature-controlled copper fixture maintained at approximately 16 °C. The input

**Fig. 3** Experimental setup for a passively Q-switched Tm:YAP laser



mirror (IM) has a 50 mm radius of curvature and is coated for anti-reflection at 793 nm and high reflectivity at 2 μm. The output mirror (OM) is flat and allows for 5% transmittance. Following the output mirror, a dichroic mirror filters out the pump wavelength while transmitting the 2 μm laser light. The output power is quantified using a Thorlabs power meter (Model S425C-L).

### 4 Results of passively Q-switched lasers

Initial experiments were conducted in continuous-wave (CW) laser mode, where, as depicted in Fig. 4a, a maximum output power of 1.73 W was achieved with an absorbed pump power of 5.58 W, resulting in a slope efficiency of 35.4%. The subsequent introduction of a TaSe<sub>2</sub> SA into the laser cavity and precise adjustment of its position enabled the attainment of passively Q-switched output (PQS), peaking at an average output power of 1.34 W and a slope efficiency of 28.3% under the same pump power conditions. Output spectrum measurements, performed with an APE WaveScan laser spectrometer having a 2 nm resolution bandwidth and shown in Fig. 4b, revealed a spectral blueshift from 1986.1 nm to 1946.7 nm during Q-switched operation, attributable to the insertion loss from the TaSe<sub>2</sub> SA which heightened the inversion level in the three-level laser system [14].

Laser pulse characteristics were monitored using an InGaAs detector (EOT, ET5000, USA) and visualized on a digital oscilloscope (Oscilloscope RTO2012, bandwidth 1 GHz, sampling rate 10Gs/s). The shortest pulse duration recorded was 550 ns at a 89 kHz repetition rate, with Fig. 5a illustrating both the profile of this pulse and a stable pulse train at the highest repetition rate. Measurements determined the single pulse energy and peak power at 15.0 μJ and 27.27 W, respectively. Figure 5b indicates a reduction in pulse width with increasing absorbed pump power, while Fig. 5c shows increases in both single pulse energy and peak power correlating with higher pump powers. Additionally, Fig. 5d displays selected outcomes for ~2 μm all-solid-state lasers employing nanomaterial-based SAs [15–22]. Among these, the TaSe<sub>2</sub> SA stands out with a remarkable average Q-switched output power of 1.34 W and a pulse duration of 550 ns, setting it apart from alternative SAs. These findings

**Fig. 4** **a** Output power **b** spectral characteristics during CW and PQS modes

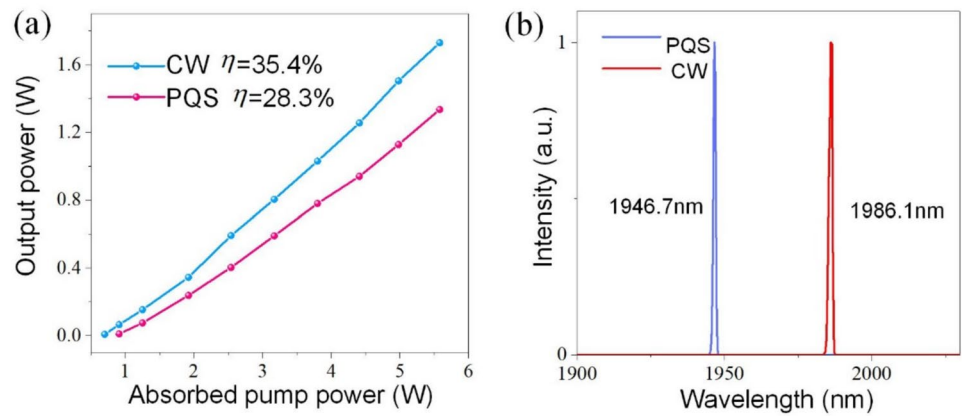
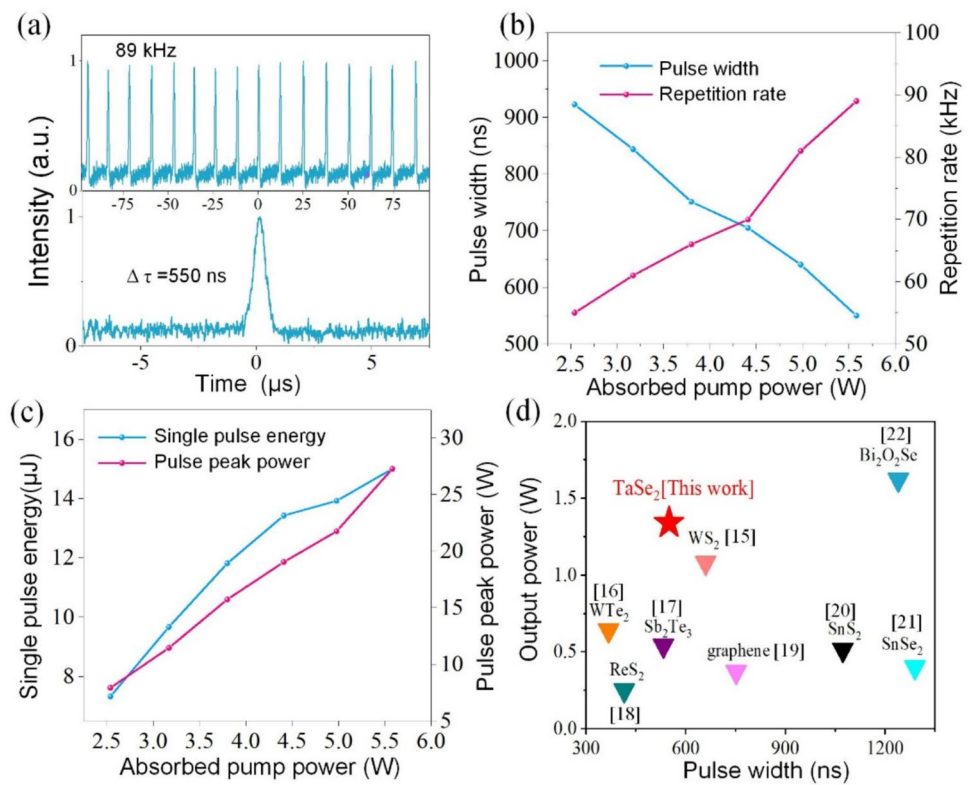


**Fig. 5** **a** Pulse train and individual pulse shape at peak absorbed pump power. **b** Variations in repetition frequency and pulse duration as a function of absorbed pump power. **c** Relationship between single pulse energy and peak power with varying absorbed pump power. **d** Outcomes from Q-switched bulk lasers in the 2.0  $\mu\text{m}$  range utilizing diverse SA



highlight TaSe<sub>2</sub>'s superior performance as an optical modulator, facilitating high Q-switched output power and notable pulse duration.

## 5 Conclusion

In this study, a high-quality TaSe<sub>2</sub> SA was fabricated using mechanical exfoliation. Its saturable absorption characteristics at 2.0  $\mu\text{m}$  were examined using an open-aperture Z-scan technique. Subsequently, the 2H-TaSe<sub>2</sub> SA was integrated into a diode-pumped, all-solid-state

passively Q-switched Tm:YAP laser. Operating from an absorbed pump power of 5.58 W, this setup achieved a maximum output power of 1.34 W at a central wavelength of 1946.7 nm. The laser produced its shortest pulse width of 550 ns at a repetition rate of 89 kHz, yielding a maximum single-pulse energy of 15.0  $\mu\text{J}$  and a peak power of 27.27 W. To our knowledge, this is the inaugural use of bilayer TaSe<sub>2</sub> as an SA for 2.0  $\mu\text{m}$  solid-state lasers. Furthermore, the results suggest that 2H-TaSe<sub>2</sub> is a viable option for generating high-power, short laser pulses, acting as an effective broadband saturable absorber.

**Acknowledgements** This work was supported by the National Natural Science Foundation of China (62205171), College Students Innovation and Entrepreneurship Training of Shandong Province (S202310429409).

**Author contributions** L.D. was responsible for performing the experiments, funding acquisition and writing the main manuscript, M.X. was responsible for investigation and aided with testing and experiments, J.L. analyzed experimental data, K.L. analyzed experimental data, J.L. was responsible for investigation, Y.J. was responsible for formal analysis, S.L. was responsible for project administration and funding acquisition.

**Data availability** No datasets were generated or analysed during the current study.

## Declarations

**Conflict of interests** The authors declare no conflict of interests.

## References

1. L. Xu, E.J. Takahashi, Dual-chirped optical parametric amplification of high-energy single-cycle laser pulses. *Nat. Photonics* **18**, 99 (2024)
2. Y.N. Zhang, K.X. Wu, Z. Guang, B. Guo, D. Qiao, Z.Y. Wei, H.Y. Yang, Q.Y. Wang, K. Li, N. Copner, X.H. Li, Advances and Challenges of Ultrafast Fiber Lasers in 2–4 μm Mid-Infrared Spectral Regions. *Laser Photonics Rev.* **18**(3), 42 (2024)
3. N. Higashitarumizu, T. Kawashima, T. Smart, R. Yalisove, C.Y. Ho, M. Madsen, D.C. Chrzan, M.C. Scott, R. Jeanloz, H. Yusa, A. Javey, Mid-Infrared, Optically Active Black Phosphorus Thin Films on Centimeter Scale. *Nano Lett.* **24**(10), 3104–3111 (2024)
4. J.T. Liu, F. Yang, J.P. Lu, S. Ye, H.W. Guo, H.K. Nie, J.L. Zhang, J.L. He, B.T. Zhang, Z.H. Ni, High output mode-locked laser empowered by defect regulation in 2D Bi<sub>2</sub>O<sub>2</sub>Se saturable absorber. *Nat. Commun.* **13**(1), 8 (2022)
5. Q.L. Bao, H. Zhang, Z.H. Ni, Y. Wang, L. Polavarapu, Z.X. Shen, Q.H. Xu, D.Y. Tang, K.P. Loh, Monolayer graphene as a saturable absorber in a mode-locked laser. *Nano Res.* **4**(3), 297–307 (2011)
6. Y. Zhang, C.Y. Ma, J.L. Xie, H. Ågren, H. Zhang, Black Phosphorus/Polymers: Status and Challenges. *Adv. Mater.* **33**(37), 2100113 (2021)
7. M. Zhang, Q. Wu, F. Zhang, L.L. Chen, X.X. Jin, Y.W. Hu, Z. Zheng, H. Zhang, 2D Black Phosphorus Saturable Absorbers for Ultrafast Photonics. *Adv. Opt. Mater.* **7**(1), 1800224 (2019)
8. S.D. Liu, Y.C. Jin, J.W. Lv, K. Li, L.L. Dong, P.F. Wang, J.T. Liu, J.P. Lu, Z.H. Ni, B.T. Zhang, High-output ~ 3 μm MIR pulsed laser enabled by surface state regulation in PtTe<sub>2</sub> optical switch. *Appl. Phys. Lett.* **124**(21), 213101 (2024)
9. W.J. Liu, L.H. Pang, H.N. Han, K. Bi, M. Lei, Z.Y. Wei, Tungsten disulphide for ultrashort pulse generation in all-fiber lasers. *Nanoscale* **9**(18), 5806–5811 (2017)
10. T. Xing, X. Wang, Z. Ou, J. Guo, D. Sun, H. Chen, X. Wang, K. Chen, Y. Gu, Peak-power of 25 W passively Q-switched ~ 28 μm Er: YAP bulk laser based on a reflective TaSe<sub>2</sub> saturable absorber mirror. *Opt. Laser Technol.* **169**, 110051 (2024)
11. S. Lim, J. Kim, C. Won, S.W. Cheong, Atomic-Scale Observation of Topological Vortices in the Incommensurate Charge Density Wave of 2H-TaSe<sub>2</sub>. *Nano Lett.* **20**(7), 4801–4808 (2020)
12. S. Chowdhury, H.M. Hill, A.F. Rigosi, A. Briggs, H. Berger, D.B. Newell, A.R.H. Walker, F. Tavazza, Examining Experimental Raman Mode Behavior in Mono- and Bilayer 2H-TaSe<sub>2</sub> via Density Functional Theory: Implications for Quantum Information Science. *ACS Appl. Nano Mater.* **4**(2), 1810–1816 (2021)
13. J.T. Liu, H. Yang, V. Khayrudinov, H. Lipsanen, H.K. Nie, K.J. Yang, B.T. Zhang, J.L. He, Ultrafast carrier dynamics and nonlinear optical response of InAsP nanowires. *Photon. Res.* **9**(9), 1811–1819 (2021)
14. X. Liu, K. Yang, S. Zhao, T. Li, W. Qiao, H. Zhang, B. Zhang, J. He, J. Bian, L. Zheng, L. Su, J. Xu, High-power passively Q-switched 2 μm all-solid-state laser based on a Bi<sub>2</sub>Te<sub>3</sub> saturable absorber. *Photon. Res.* **5**(5), 461–466 (2017)
15. C. Luan, K.J. Yang, J. Zhao, S.Z. Zhao, L. Song, T. Li, H.W. Chu, J.P. Qiao, C. Wang, Z. Li, S.Z. Jiang, B.Y. Man, L.H. Zheng, WS<sub>2</sub> as a saturable absorber for Q-switched 2 micron lasers. *Opt. Lett.* **41**(16), 3783–3786 (2016)
16. L.J. Chen, X. Li, H.K. Zhang, W. Xia, Passively Q-switched 1.989 μm all-solid-state laser based on a WTe<sub>2</sub> saturable absorber. *Appl. Opt.* **57**(35), 10239–10242 (2018)
17. X.H. Wang, J.Y. Hu, J.L. Xu, Y.J. Sun, H.P. Xia, C.Y. Tu, Sb<sub>2</sub>Te<sub>3</sub> as the saturable absorber for the ~2.0 μm passively Q-switched solid state pulsed laser. *RSC Adv.* **9**(50), 29312–29316 (2019)
18. X.C. Su, B.T. Zhang, Y.R. Wang, G.B. He, G.R. Li, N. Lin, K.J. Yang, J.L. He, S.D. Liu, Broadband rhenium disulfide optical modulator for solid-state lasers. *Photonics Research* **6**(6), 498–505 (2018)
19. Z. Cui, B.Q. Yao, X.M. Duan, Y.Y. Li, J.H. Yuan, T.Y. Dai, A graphene saturable absorber for a Tm:YLF pumped passively Q-switched Ho:LuAG laser. *Optik* **127**(5), 3082–3085 (2016)
20. Z.C. Shi, X.H. Sun, W.Q. Xie, P.H. Chang, S.W. Li, L.M. Zhang, X.T. Yang, Passively Q-switched Tm:YAP laser based on SnS<sub>2</sub> saturable absorber. *Optik* **264**, 169421 (2022)
21. X.C.A. Liu, Q. Yang, C.H. Zuo, Y.P. Cao, X.L. Lun, P.C. Wang, X.Y. Wang, 2-μm passive Q-switched Tm:YAP laser with SnSe<sub>2</sub> absorber. *Opt. Eng.* **57**(12), 126105 (2018)
22. R. Zhang, J.Q. Xun, M.Y. Shao, H.Z. Ma, X.H. Sun, F.J. Tian, Z.C. Shi, X.T. Yang, A 1.62-W passively Q-switch Tm<sup>3+</sup> doped laser with a Bi<sub>2</sub>O<sub>2</sub>Se saturable absorber. *Microw. Opt. Technol. Lett.* **65**(5), 1410–1414 (2023)

**Publisher's Note** Springer Nature remains neutral with regard to jurisdictional claims in published maps and institutional affiliations.

Springer Nature or its licensor (e.g. a society or other partner) holds exclusive rights to this article under a publishing agreement with the author(s) or other rightsholder(s); author self-archiving of the accepted manuscript version of this article is solely governed by the terms of such publishing agreement and applicable law.